CHAPTER IV
RESULTS AND DISCUSSION

4.1 Preparation and Characterization of as-spun PBSu-DCH fibers

4.1.1 Effect of Polymer Concentration on as-spun fibers

The effect of polymer concentration on morphological appearance and size of the as-spun fibers was investigated by varying concentration of PBSu-DCH solutions at a given applied electrical potential and collection distance.

Figure 4.1 shows SEM images of as-spun fibers from 18, 20, 22, and 24% w/v over a fixed applied electrical potential of 17 kV and collection distance of 20 cm. When the PBSu-DCH concentration was 18% w/v, a combination between beads and fibers was observed (figure 4.1-a). At low concentrations of the spinning solutions, surface tension is the dominant factor. In such circumstances, the solutions did not have chain entanglement to withstand the force acting on the jet. Once the charged jet was broken up, surface tension resulted in the formation of discrete droplets. Increased the polymer concentration to 20% w/v, the bead fraction decreased resulting in more uniform fibers deposited on the collector screen because chain entanglement high enough to prevent the breaking of the charged jet (figure 4.1-b). When the PBSu-DCH concentration further increased to 22% w/v, smooth fibers without the presence of beads were observed (figure 4.1-c). Although, when the PBSu-DCH concentration was 24% w/v, the bead-liked fibers appeared again (figure 4.1-d).

For a given applied electrical potential and collection distance, the diameters of the as-spun fibers increased with increasing concentration of PBSu-DCH solutions, a direct result of the increase in viscosity of the spinning dopes. The increased concentration enabled the charged jet withstand a larger stretching force (from the Coulombic repulsion). The average diameter of the obtained fibers increased from about 159±10 nm when the PBSu-DCH concentration was 18%w/v to about 248±8.2 nm when the PBSu-DCH concentration was 24%w/v.
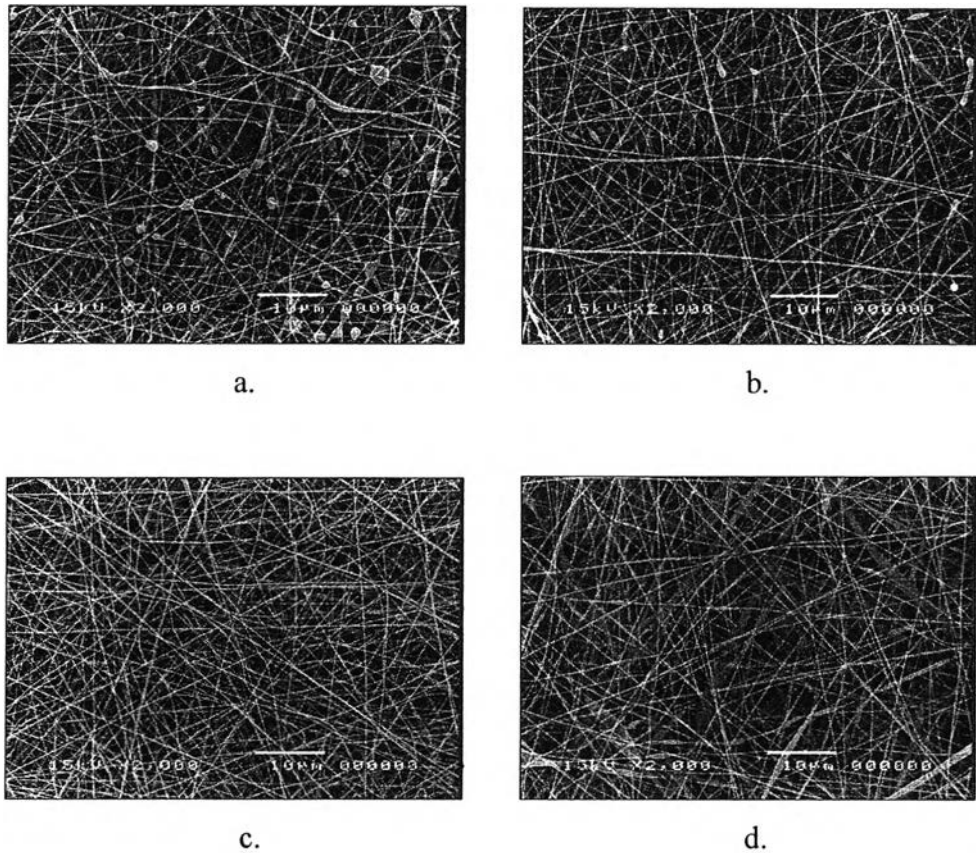
a.

b.

c.

d.

Figure 4.1 Selected SEM images (scale bar = 10μm and magnification = 2000x) illustrating the effect of solution concentration on morphology of PBSu-DCH fibers that were electrospun from PBSu-DCH solutions in dichloromethane/trifluoroacetic acid (90/10) at various concentrations. PBSu-DCH concentrations were 18% w/v (panel a), 20% w/v (panel b), 22% w/v (panel c), and 24% w/v (panel d).

4.1.2 Effect of Collection Distance and Applied Electrical Potential

Effect of collection distance and applied electrical potential on the morphological appearance and size of the as-spun fibers was investigated. 22% w/v PBSu-DCH solution was electrospun under an applied potential of 14, 17, and 20 kV over a collection distance of 15, 20, and 25 cm. For a given concentration and collecting distance, increasing applied electrical potential caused the fiber diameters to decrease and smooth fibers without the presence of beads were obtained at applied electrical potential of 17 kV. With increasing collection distance, the average diameter of the as-spun fibers was found to decrease from about 249±0.5 nm at the

collection distance of 15 cm to about 144±0.9 nm at the collection distance of 25 cm. Increased in collection distance for a fixed applied electrical potential resulted in the decreasing in electrostatic field strength, so electrostatic forces exerting on a jet decreased. The decreased electrostatic forces cause the jet to exhibit the bending instability closer to the nozzle tip, resulting in the actual trajectory of the jet to increase appreciably (i.e. the looping trajectory) (Reneker *et al.*, 2000; Mit-uppatham *et al.*, 2004). Increasing in the path trajectory allows the jet to elongate and thin down in a greater extent prior to solidifying. In the case where beaded fibers were obtained, the shorter path length for traveling to the target causes the fibers having not enough time to elongate and solidify, resulting in the bead-liked fibers depositing on the target.

Table 4.1 shows SEM images of PBSu-DCH fibers at 22% w/v PBSu-DCH in dichloromethane/trifluoroacetic acid (90/10) at various applied electrical potential (kV) and collection distance (cm). Among the various spinning conditions investigated, 22% w/v PBSu-DCH solution at the applied electrical potential of 17 kV and a collection distance of 20 cm was chosen as the optimum condition for further study (see Figure 4.2). Diameters of the as-spun fibers were measured directly from the SEM images of 10,000X magnification using a SemAphore 4.0 software, with the average value being calculated from at least 100 measurements. The average diameter of the obtained as-spun PBSu-DCH fibers was 172±3.4 nm.
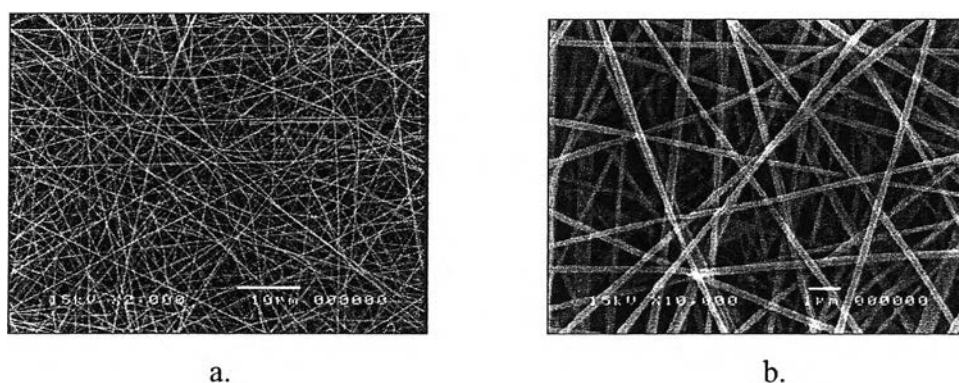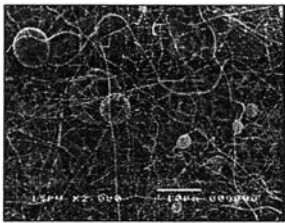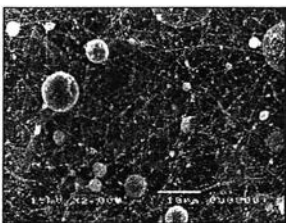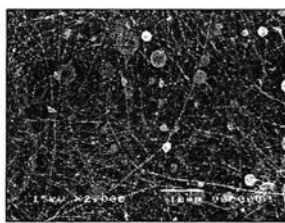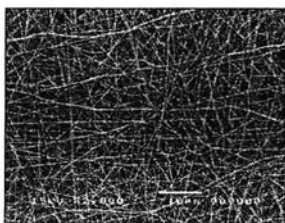

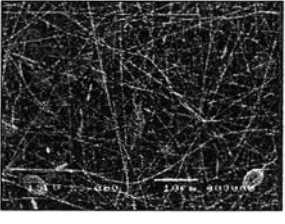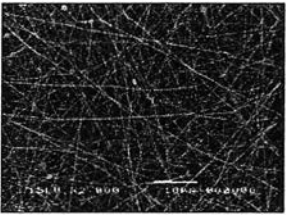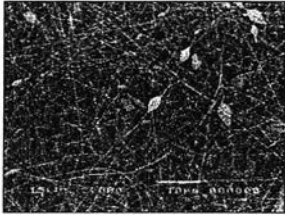a.   b.
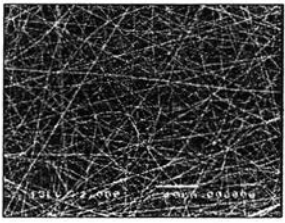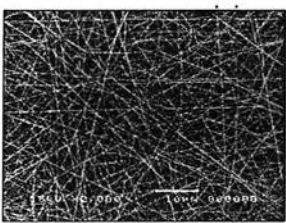
Figure 4.2 SEM images of the as-spun PBSu-DCH fibers from 22% w/v PBSu-DCH solution at the applied electrical potential of 17 kV and a collection distance of 20 cm. a. magnification of 2,000 b. magnification of 10,000

Table 4.1 SEM images of as-spun PBSu-DCH fibers from 22 % w/v PBSu-DCH in dichloromethane/trifluoroacetic acid (90/10) at various applied electrical potential (kv) and collection distance (cm)

Distance (cm)	Applied Voltage (kV)		
	14	17	20
15			
20			
25			

4.2 Mechanical and Physical Characteristics of the as-spun PBSu-DCH Fibers

The mechanical integrity of the electrospun fibrous scaffolds in comparison with that of the solution-cast film scaffolds was also investigated for a better understanding of the potential use the electrospun fibers as scaffolds for tissue engineering. To investigate the mechanical integrity of the fibrous scaffolds in terms of tensile strength, Young's modulus, and elongation at break of both fibrous and

film scaffolds, the spinning solutions were electrospun for 10 hr to obtain as-spun mats that were about 120 μm in thickness. The obtained results are summarized in table 4.2.

Table 4.2 Mechanical characteristics of the as-spun PBSu-DCH fiber mats of about 120 μm thick as well as those of solution-cast film of PBSu-DCH

Mechanical Properties	Solution-cast Films	As-spun Fiber mats
Tensile strength at break (MPa)	2.93	1.17
Tensile strength at break/density [a] (MPa·cm^3·g^{-1})	2.06	2.88
Tensile strength at yield (MPa)	24.38	10.14
Tensile strength at yield/density [a] (MPa·cm^3·g^{-1})	17.17 · .	.24.97
Young's modulus (MPa)	616.96	43.43
Elongation at break (%)	46.95	121.71

[a] Density of the as-spun PBSu-DCH fiber mats (i.e. 0.406 g/cm^3) and the solution-cast films of PBSu-DCH (i.e. 1.42 g/cm^3) were measured by a Sartorius YDK01 measurement.

The specific tensile strength at break/density of the as-spun PBSu-DCH scaffolds was about 2.88 MPa, while that of the film scaffolds was lower than that of the as-spun one, with the property value about 2.06 MPa. With regard to the Young's modulus, the fibrous scaffolds exhibited the property value lower than that of the film one. Mechanically, great improvement of the elongation at break was observed for the as-spun fibrous scaffolds as shown in table 4.2 that the fibrous scaffolds exhibited much greater elongation at break than that of the film one. The results indicated that the electrospun fibrous scaffolds are soft and tough, in contrast to the hard and brittle solution-cast films. In addition, the porosity (ε) of the fibrous scaffolds was investigated base on the different between the density of PBSu-DCH

(i.e. about 1.3 g/cm^3) and the density of the as-spun fibrous scaffolds (i.e. 0.406 g/cm^3) to be about 68.7%.

4.3 Thermal Characteristics of the as-spun PBSu-DCH Fibers

Thermal properties of the as-spun fibers and solution-cast films of PBSu-DCH including those of the as-received PBSu-DCH pellets were characterized using differential scanning calorimeter (DSC) and thermogravimetric/differentialthermal analyzer (TGA). In DSC, the scanning program consists of four stages. Each sample was first heated from 25 to 150°C (HEAT 1) to observe the melting behavior of the original crystalline of each sample and then annealed at 150°C for 5 min to erase any thermal history. After melt-annealing, the sample was cooled down to 25°C (COOL) to observe the ability of the sample to crystallize when it was subjected to a constant cooling scan. For the last stage, the sample was reheated to 150°C (HEAT 2) in order to observe the melting behavior of the sample which was formed during the constant cooling scan. The experimental results of thermal characteristics and crystallinity of the samples are summarized in table 4.3.

In the first stage (HEAT 1), the apparent melting temperature (T_m) of the as-spun fibers and solution-cast film of PBSu-DCH as well as those of the as-received pellets was observed at 113.61, 111.19, and 114.06°C, respectively. The apparent degree of crystallinity of each sample was calculated from the apparent enthalpy of fusion (ΔH_f) as obtained from HEAT 1. The results showed that the as-received pellets and solution-cast films of PBSu-DCH exhibited the degree of crystallinity of 77.03 and 86.38 %, respectively, whereas the as-spun fibers exhibited lower values at 66.9 %. The observed lower degree of crystallinity of the as-spun fibers in comparison with those of the as-received pellets and solution-cast films should be a result of the rapid solidification process during the later stage of electrospinning. This can be understood as the rapid solidification process may hinder the development of crystallinity as the chains do not have enough time to form crystalline registration. The retardation of crystallization due to electrospinning has been first reported by Liu et al., (2005). Due to the one-dimensional fiber size effect, the growth of crystalline phase on the radial direction of the fibers was restrained.

The melting heat of the electrospun fibrous membrane was smaller than that of the cast membrane by a reason of rapid solification and restricted crystalline structure (Cheng et al., 2008). The thermal behavior of stage III (COOL) was also studied. The crystallization temperature (T_c) of the as-spun scaffolds, the solution-cast films, and the as-received pellets of PBSu-DCH were observed at 76.36, 83.31, and 84.58°C, respectively.

In the subsequent heating (HEAT 2), double melting phenomenon was evident for all samples. As in the case of poly(trimethylene terephthalate) (PTT), Srimoaon et al.,2004 reported that the occurrence of the lower melting endotherm was a result of the melting of the primary crystallites formed during previous cooling, while that of the higher melting endotherm corresponded to the melting of the recrystallized crystallites formed during subsequent heating scan.

Analysis of DSC showed that electrospinning procedure seems to reduce the thermal properties of PBSu-DCH. According to the results in table 4.3, T_m, T_c, and ΔH_f values for PBSu-DCH pellets are 114.06, 84.58, and 85.12, respectively. TGA was also performed in order to investigate thermal degradation of these samples. The results showed that thermal degradation temperature (T_d) of the as-spun fibers, the solution-cast films, and the as-received pellets of PBSu-DCH were found to be quite comparable (i.e. 381.4, 379, and 380.5°C, respectively).

Table 4.3 Thermal characteristics of the electrospun fiber mats and solution-cast film of PBSu-DCH as well as those of the as-received pellets of PBSu-DCH

Thermal Properties	Electrospun fibers	Solution-cast films	As-received pellets
Melting Temperature, T_m (°C)	113.61	111.19	114.06
Crystallization Temperature, T_c (°C)	76.36	83.31	84.58
Degradation Temperature, T_d (°C)	381.47	379.07	380.51
Apparent enthalpy of fusion, ΔH_f (J/g)	73.93	96.87	85.12
Degree of crystallinity, %	66.9	86.38	77.03

4.4 Cell Study

The potential use of the as-spun PBSu-DCH fiber mats as scaffolds for bone regeneration with respect to that of the solution-cast films was evaluated *in vitro* with human osteoblasts (SaOS-2) and mouse fibroblasts (L929) in terms of biocompatibility, attachment, proliferation, and ALP activity of cultured cells.

4.4.1 Indirect Cytotoxicity Evaluation

Biocompatibility of the as-spun PBSu-DCH fiber mats were evaluated based on indirect cytotoxicity test using human osteoblasts (SaOS-2) and mouse fibroblasts (L929) as reference cells. Figure 4.3 shows the absorbance obtained from MTT assay of the cells which were cultured with the extraction media from fibrous PBSu-DCH scaffolds in comparison with those cultured with SFM (i.e. control). The experimental results show that, for both SaOS-2 and L929, film and fibrous scaffolds of PBSu-DCH exhibited comparable average absorbance values, in comparison with those of the control. The obtained results revealed that the electrospun mats of PBSu-DCH were non-toxic to both types of cells and could be useful as bone scaffolds.
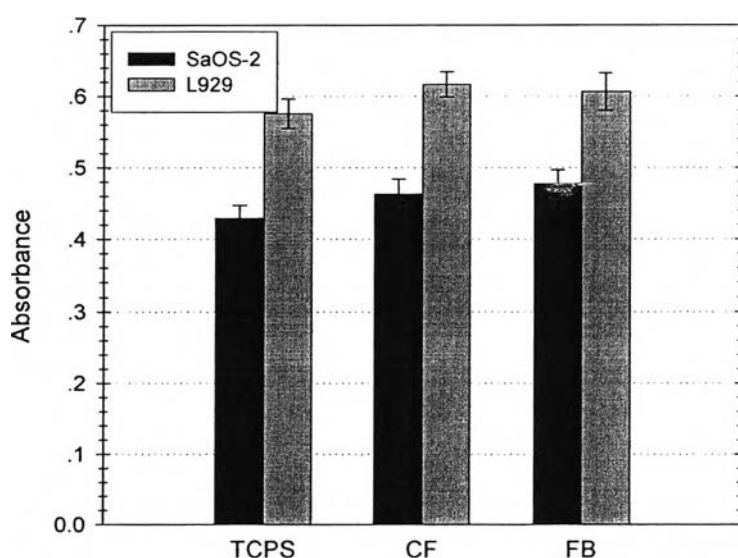
Figure 4.3 Indirect cytotoxic evaluation of TCPS (controls), and film and fibrous PBSu-DCH scaffolds based on viability of human osteoblasts (SaOS-2) and mouse fibroblasts (L929).

4.4.2 Cell Attachment and Proliferation

Attachment and proliferation of cells are the important aspects of scaffolding materials. In this work, the as-spun PBSu-DCH fibrous scaffolds were evaluated in comparison with film scaffolds and TCPS. To evaluate cellular behavior on TCPS (i.e. controls), film, and fibrous scaffolds, SaOS-2 cells were seeded and cultured on all substrates. The number of cells attached on both types of scaffolds and TCPS could be quantified by the UV absorbance from MTT assay. Figure 4.4 shows attachment and proliferation of SaOS-2 on TCPS (i.e. controls), and film and fibrous scaffolds of PBSu-DCH as a function of time in culture.
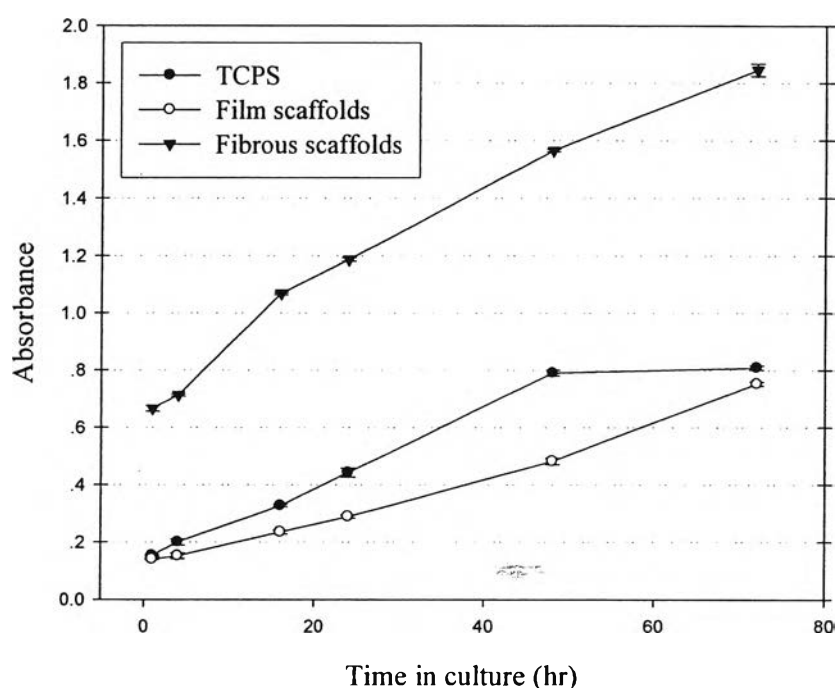
Figure 4.4 Attachment and proliferation of SaOS-2 on TCPS, and film and fibrous scaffolds of PBSu-DCH as a function of time in culture.

The results show that the attachment of SaOS-2 on fibrous scaffolds was much greater than that on the film scaffolds and TCPS. After 4 hr in culture, the attachment of SaOS-2 on the fibrous scaffolds increased significantly, while the amount of cell adhesion on film scaffolds and TCPS increased slowly with time. This result could be related to the increasing in surface area of the fibrous scaffolds that

provides more available surface for the attachment of cells on the materials in comparison with film scaffolds.
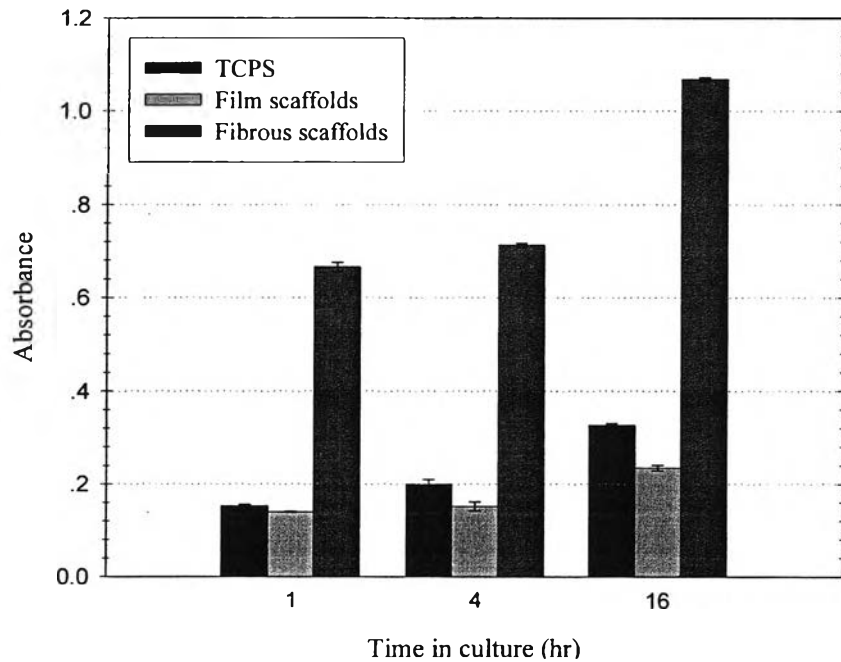
Figure 4.5 Attachment of SaOS-2 on TCPS, and film and fibrous scaffolds of PBSu-DCH as a function of time in culture.

For further evaluation to assess whether the as-spun PBSu-DCH fiber mats could be used as bone scaffolding materials, the proliferation of SaOS-2 on TCPS (i.e. controls), and film and fibrous scaffolds of PBSu-DCH at day 1,2, and 3 after being allowed for cell attachment for 16 hr is illustrated in figure 4.6.

Apparently, the proliferation of SaOS-2 on the fibrous scaffolds was much better than that on the film scaffolds and TCPS. Between day 1 and 2, all of the substrates showed a high proliferation rate. Interestingly, after longer culturing times (i.e. 48 and 72 hr), the proliferation of SaOS-2 on fibrous and film scaffolds still continuously increased with time, whereas the proliferation of the cells on TCPS was found to be constant after 2 days in culture. The saturation in the viability of the cells could be a result of the differentiation of the cells. The explanation for the observed much better proliferation of the cells on the fibrous scaffolds than that on the film

scaffolds and TCPS could be the high porosity of the fibrous scaffolds that provides large surface area for cell incorporation and propagation.
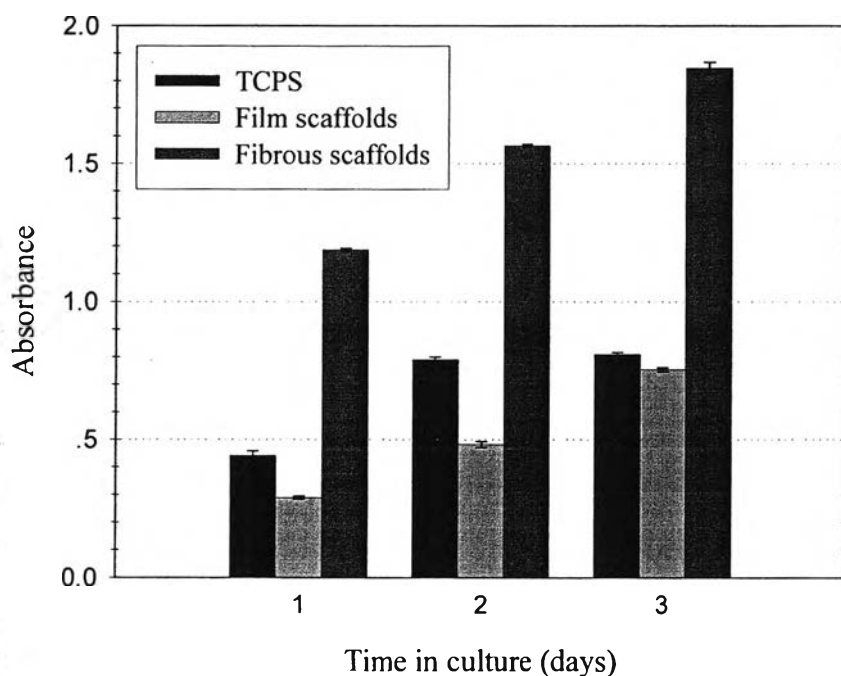
Figure 4.6 Proliferation of SaOS-2 on TCPS, and film and fibrous scaffolds of PBSu-DCH as a function of time in culture.

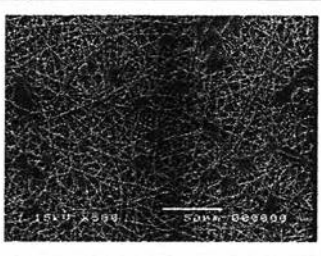SEM observations were carried out in order to observe cell morphology and interaction between cells and cells and the scaffolds. SEM images of SaOS-2 that were cultured on the fibrous and film scaffolds of PBSu-DCH, and a glass substrates (i.e. controls) at a different time in culture were shown in table 4.4, 4.5, and 4.6, respectively. These SEM images confirmed that the phenotype of SaOS-2 was maintained during the cell culture. Interestingly, the cells that were cultured on the fibrous scaffolds exhibited the expanded shape with discrete branches to help attach themselves on the fiber surfaces after only about 1 hr in culture, while those cultured on film scaffolds and glass substrates were still round. At longer culturing times, the cells on the fibrous scaffolds expanded even more and could penetrate into the inner side of the scaffolds very well. For film scaffolds and glass substrates, the

cells started to expand and elongate after about 4 hr. At 16 hr in culture, the cells on film scaffolds and glass substrates changed from round shape to elongated and spindle-like shape and also expanded even more at longer time in culture.

According to the results obtained, the as-spun fibrous scaffolds of PBSu-DCH have an ability to promote both the attachment and proliferation of SaOS-2 particularly well. This evident implies the possibility of using the as-spun PBSu-DCH fiber mats as bone scaffolds.

4.4.3 Alkaline Phosphatase (ALP) Activity

In addition to attachment and proliferation, the ability to support cells differentiation of a scaffold is another important aspect. In this work, SaOS-2 were cultured on scaffolds specimens for 3, 5, and 10 days to observe the production of alkaline phosphatase (ALP) which is an important indicator determining the activity of cells on the scaffolds. Figure 4.7 shows the ALP activity of SaOS-2 cultured on TCPS (i.e. controls), and film and fibrous scaffolds of PBSu-DCH after 3, 5, and 10 days in culture. Evidently, for all of the substrates investigated, the ALP activity increased with increasing time in culture. The ALP activity on different substrates can be ranked as followed: TCPS > fibrous scaffolds > film scaffolds. In comparison with other substrates, TCPS exhibited the highest ALP activity of SaOS-2. The reason for this should be due to the fact that proliferation of the cells on TCPS, after 2 days in culture, was found to be constant, while that on the fibrous and film scaffolds investigated still increased steadily. According to figure 4.4, the proliferation rate of the cells cultured on TCPS reached a plateau after days 2. If we are to assumed that the differentiation should begin as soon as the proliferation rate starts to decrease (Stein *et al.*,1990), the amount of ALP synthesized from the cells on TCPS after 2 days in culture should be the highest, which is what has been observed in this work. According to figure 4.4, the obtained result shows that the cells that were cultured on the as-spun fibrous scaffolds exhibited the higher ALP activity than that on the film scaffolds. This evident suggests that the fibrous scaffolds could promote cell proliferation and differentiation of SaOS-2 particularly well.

Table 4.4 Selected SEM images of SaOS-2 cultured on fibrous scaffolds of PBSu-DCH as a function of time in culture
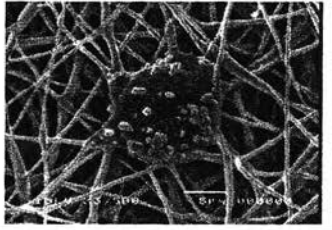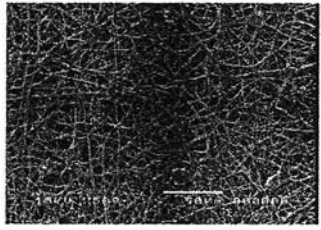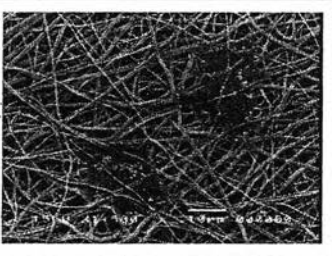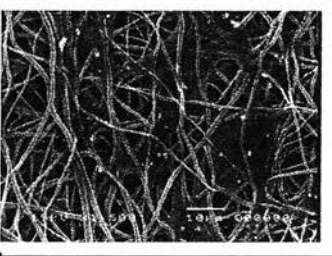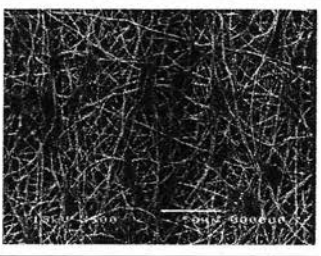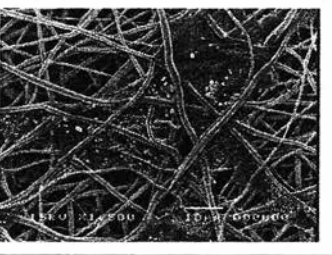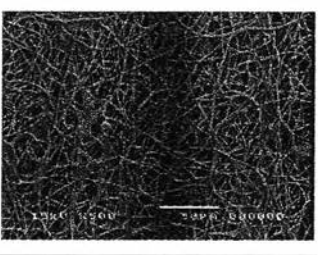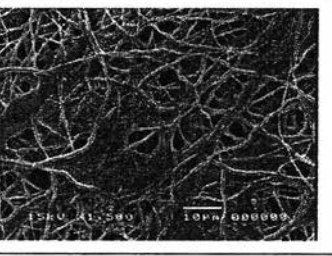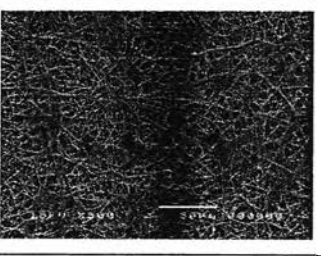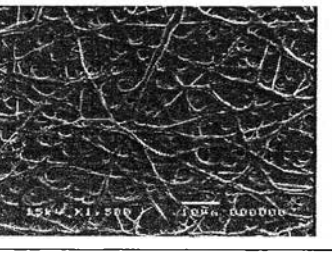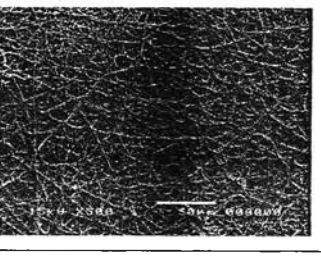
Time in Culture (hr)	High-magnification	Low-magnification
1		
4		
16		
24		
48		
72		

Table 4.5 Selected SEM images of SaOS-2 cultured on film scaffolds of PBSu-DCH as a function of time in culture
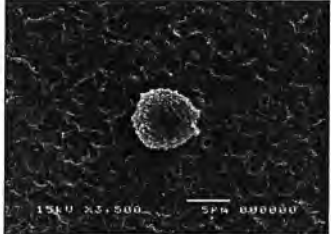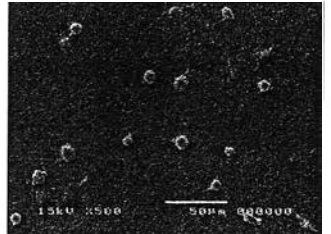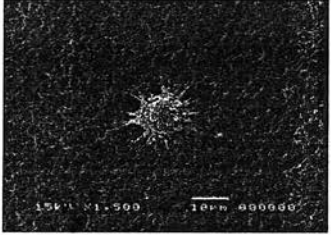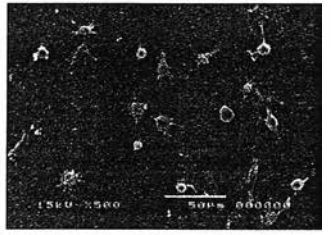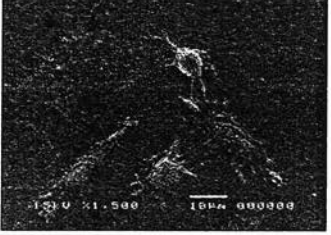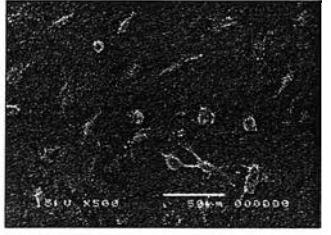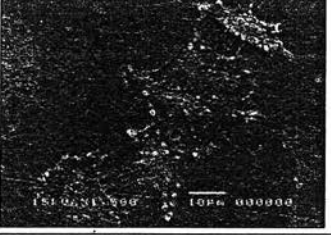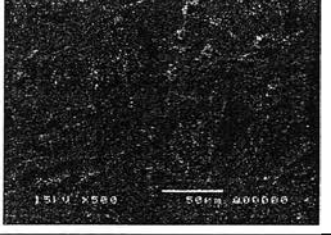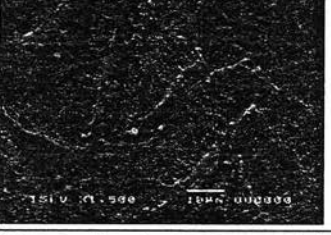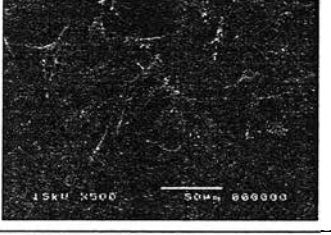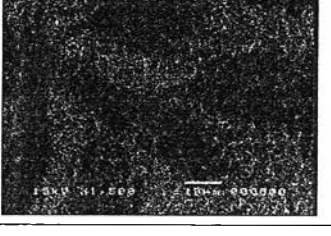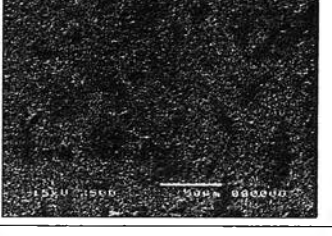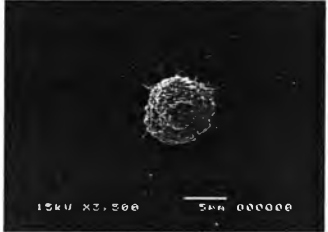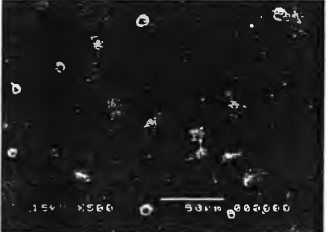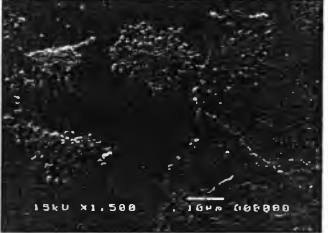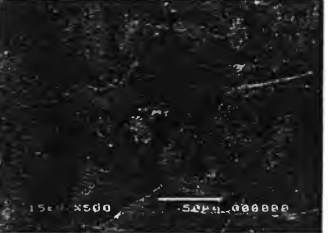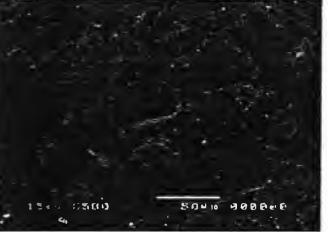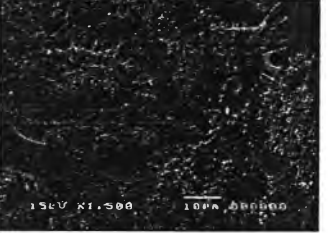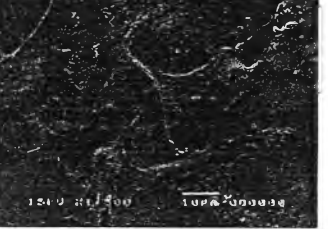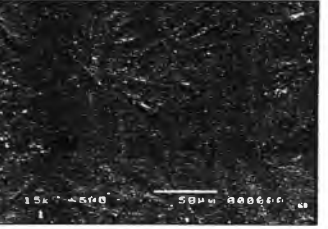
Time in Culture (hr)	High-magnification	Low-magnification
1		
4		
16		
24		
48		
72		

Table 4.6 Selected SEM images of SaOS-2 cultured on glass substrates as a function of time in culture

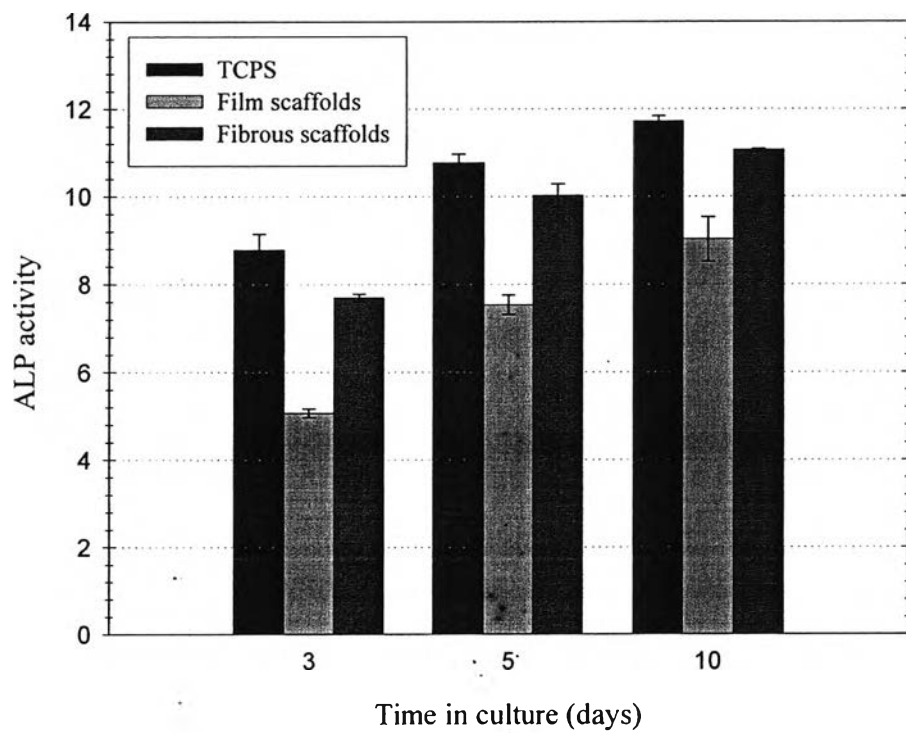| Time in Culture (hr)	High-magnification	Low-magnification
1		
4		
16		
24		
48		
72		

Figure 4.7 ALP activity of SaOS-2 cultured on TCPS (i.e. controls), and film and fibrous scaffolds of PBSu-DCH after 3, 5, and 10 days in culture.